

STUDY ON THE STABILITY AND NUMERICAL ERROR OF THE FOUR-STAGES SPLIT-STEP FDTD METHOD INCLUDING LUMPED INDUCTORS

Y.-D. Kong¹, Q.-X. Chu^{1, 2, *}, and R.-L. Li¹

¹School of Electronic and Information Engineering, South China University of Technology, Guangzhou, Guangdong 510640, China

²The State Key Laboratory of Millimeter Waves, Nanjing, Jiangsu 210096, China

Abstract—The stability and numerical error of the extended four-stages split-step finite-difference time-domain (SS4-FDTD) method including lumped inductors are systematically studied. In particular, three different formulations for the lumped inductor are analyzed: the explicit, the semi-implicit, and the implicit schemes. Then, the numerical stability of the extended SS4-FDTD method is analyzed by using the von Neumann method, and the results show that the proposed method is unconditionally-stable in the semi-implicit and the implicit schemes, whereas it is conditionally stable in the explicit scheme, which its stability is related to both the mesh size and the values of the element. Moreover, the analysis of the numerical error of the extended SS4-FDTD is studied, which is based on the Norton equivalent circuit. Theoretical results show that: 1) the numerical impedance is a pure imaginary for the explicit scheme; 2) the numerical equivalent circuit of the lumped inductor is an inductor in parallel with a resistor for the semi-implicit and implicit schemes. Finally, a simple microstrip circuit including a lumped inductor is simulated to demonstrate the validity of the theoretical results.

1. INTRODUCTION

The finite-difference time-domain (FDTD) method [1] has been proven to be an established numerical technique that provides accurate predictions of field behaviors for electromagnetic interaction problems. However, the applications of the FDTD method had been restricted

Received 20 June 2012, Accepted 5 September 2012, Scheduled 20 September 2012

* Corresponding author: Qing-Xin Chu (qxchu@scut.edu.cn).

by the well-known Courant-Friedrichs-Lewy (CFL) condition [2] on the time step and the numerical dispersion associated with space discretization.

Recently, to overcome the CFL condition on the time step size of the FDTD method, an unconditionally-stable FDTD method based on the alternating direction implicit (ADI) technique was developed [3, 4]. The ADI-FDTD method has second-order accuracy both in time and space. Nevertheless, it presents large numerical dispersion error with large time steps. Then, improved ADI-FDTD methods were proposed [5, 6]. Subsequently, other unconditionally-stable methods such as Crank-Nicolson based [7–10], split-step [11, 12] and locally-one dimensional (LOD) [13, 14] FDTD methods were developed. The LOD-FDTD method can be considered as the split-step approach (SS1) with first-order accuracy in time, which consumes less CPU time than that of the ADI-FDTD method. Then, fourth-order LOD-FDTD was presented in [15]. Moreover, three-dimensional LOD-FDTD methods with second-order accuracy in time were shown in [16, 17]. To reduce the dispersion error, an efficient six-stages split-step unconditionally-stable FDTD method was proposed in [18]. Furthermore, to improve the accuracy, unconditionally-stable FDTD methods with high-order accuracy and low dispersion error in 2-D domains were proposed in [19–21]. Then the method in [19] was extended to 3-D domains, and high-order split-step unconditionally-stable FDTD was proposed in [22], which denoted as SS4-FDTD herein.

Along another line, there have been many efforts made for the extended FDTD [23–26] to incorporate the passive and active lumped elements into FDTD method. Through the stability analysis of the extended FDTD methods in recent years [27–29], one can find that the stability of the previous extended FDTD including passive lumped elements is either related to the mesh size, or related to both the mesh size and the values of the elements. Furthermore, an unconditionally stable FDTD technique including passive lumped elements based on the Crank-Nicolson method was presented in [30]. An unconditionally stable ADI-FDTD method including passive lumped elements was proposed in [31], and the stability analysis was given based on the energy concept. Subsequently, the numerical dispersion of the ADI-FDTD technique including lumped models was studied based on the circuitual viewpoint [32]. The LOD-FDTD method was extended to include lumped elements [33]. However, the unconditionally-stable SS4-FDTD method has not been extended to include lumped elements, then the study on its stability and numerical error is very useful.

The stability and numerical error of the extended four-stages split-step finite-difference time-domain (SS4-FDTD) method including

lumped inductors are systematically studied in this paper. Firstly, the formulation of the extended SS4-FDTD method is given. Specially, three different formulations for the lumped inductor are analyzed: the explicit, the semi-implicit, and the implicit schemes. Secondly, the numerical stability of the extended SS4-FDTD method is analyzed by using the von Neumann method, and the results show that the proposed method is unconditionally-stable in the semi-implicit and the implicit schemes, whereas it is conditionally stable in the explicit scheme. Thirdly, the numerical error analysis of the extended SS4-FDTD is studied, which based on the Norton equivalent circuit. Theoretical results show that: the numerical equivalent circuit of the lumped inductor is an inductor in parallel with a resistor for the semi-implicit and the implicit schemes. Finally, a simple microstrip circuit including a lumped inductor is simulated to demonstrate the validity of the theoretical results.

2. FORMULATION OF THE EXTENDED SS4-FDTD METHOD

In linear, isotropic, non-dispersive and lossless medium, ε and μ are the electric permittivity and magnetic permeability, respectively. The lumped inductor is replaced along the $+z$ direction and the contribution of the lumped inductor is presented by \vec{J}_{Lz} . Then, the 3-D Maxwell's equations can be written in a matrix form as

$$\partial\vec{u}/\partial t = [M] \vec{u} - \vec{J}_{Lz}/\varepsilon. \quad (1)$$

where $\vec{u} = [E_x, E_y, E_z, H_x, H_y, H_z]^T$, and $[M]$ is the Maxwell's matrix.

Symmetric operator and uniform splitting are simultaneously exploited to decompose the matrix $[M]$ into four parts. Then, (1) can be written as

$$\partial\vec{u}/\partial t = [A]/2 \cdot \vec{u} + [B]/2 \cdot \vec{u} + [A]/2 \cdot \vec{u} + [B]/2 \cdot \vec{u} - \vec{J}_{Lz}/\varepsilon. \quad (2)$$

Due to the limitation of space, $[M]$, $[A]$, and $[B]$ are not shown here. They can be found in [21].

By using the split-step scheme [34], (2) is divided into four sub-equations, from n to $n+1$, one time step is divided into four sub-steps accordingly, $n \rightarrow n+1/4$, $n+1/4 \rightarrow n+2/4$, $n+2/4 \rightarrow n+3/4$ and $n+3/4 \rightarrow n+1$, by successively solving

$$\text{sub-step 1: } \partial\vec{u}/\partial t = 4 \cdot \left([A]/2 \cdot \vec{u} - \vec{J}_{Lz}/4\varepsilon \right) \quad n \rightarrow n+1/4 \quad (3a)$$

$$\text{sub-step 2: } \partial\vec{u}/\partial t = 4 \cdot \left([B]/2 \cdot \vec{u} - \vec{J}_{Lz}/4\varepsilon \right) \quad n+1/4 \rightarrow n+2/4 \quad (3b)$$

$$\text{sub-step 3: } \partial \vec{u} / \partial t = 4 \cdot \left([A] / 2 \cdot \vec{u} - \vec{J}_{Lz} / 4\epsilon \right) \quad n+2/4 \rightarrow n+3/4 \quad (3c)$$

$$\text{sub-step 4: } \partial \vec{u} / \partial t = 4 \cdot \left([B] / 2 \cdot \vec{u} - \vec{J}_{Lz} / 4\epsilon \right) \quad n+3/4 \rightarrow n+1. \quad (3d)$$

Furthermore, the right side of the above equations can be approximated by using the Crank-Nicolson scheme [7]. Subsequently, four sub-procedures are generated as follows

$$([I] - \Delta t / 4 \cdot [A]) \vec{u}^{n+1/4} = ([I] + \Delta t / 4 \cdot [A]) \vec{u}^n - \Delta t \vec{J}_{Lz}^{n+1/8} / 4\epsilon \quad (4a)$$

$$([I] - \Delta t / 4 \cdot [B]) \vec{u}^{n+2/4} = ([I] + \Delta t / 4 \cdot [B]) \vec{u}^{n+1/4} - \Delta t \vec{J}_{Lz}^{n+3/8} / 4\epsilon \quad (4b)$$

$$([I] - \Delta t / 4 \cdot [A]) \vec{u}^{n+3/4} = ([I] + \Delta t / 4 \cdot [A]) \vec{u}^{n+2/4} - \Delta t \vec{J}_{Lz}^{n+5/8} / 4\epsilon \quad (4c)$$

$$([I] - \Delta t / 4 \cdot [B]) \vec{u}^{n+1} = ([I] + \Delta t / 4 \cdot [B]) \vec{u}^{n+3/4} - \Delta t \vec{J}_{Lz}^{n+7/8} / 4\epsilon. \quad (4d)$$

where $[I]$ is a 6×6 identity matrix. Without loss of generality, the updating equations are herein presented for the sub-step 1 only. More specifically, (4a) can be rewritten as

sub-step 1:

$$E_x^{n+1/4} = E_x^n + \frac{\Delta t}{4\epsilon} \frac{\partial}{\partial y} \left(H_z^{n+1/4} + H_z^n \right) \quad (5a)$$

$$E_y^{n+1/4} = E_y^n + \frac{\Delta t}{4\epsilon} \frac{\partial}{\partial z} \left(H_x^{n+1/4} + H_x^n \right) \quad (5b)$$

$$E_z^{n+1/4} = E_z^n + \frac{\Delta t}{4\epsilon} \frac{\partial}{\partial x} \left(H_y^{n+1/4} + H_y^n \right) - \frac{\Delta t}{4\epsilon} J_{Lz}^{n+1/8} \quad (5c)$$

$$H_x^{n+1/4} = H_x^n + \frac{\Delta t}{4\mu} \frac{\partial}{\partial z} \left(E_y^{n+1/4} + E_y^n \right) \quad (5d)$$

$$H_y^{n+1/4} = H_y^n + \frac{\Delta t}{4\mu} \frac{\partial}{\partial x} \left(E_z^{n+1/4} + E_z^n \right) \quad (5e)$$

$$H_z^{n+1/4} = H_z^n + \frac{\Delta t}{4\mu} \frac{\partial}{\partial y} \left(E_x^{n+1/4} + E_x^n \right). \quad (5f)$$

To account for lumped inductors, the constitutive equation of the inductors can be considered, in differential

$$\frac{dI_{Lz}}{dt} = \frac{1}{L} V_z. \quad (6)$$

or integral form

$$I_{Lz} = \frac{1}{L} \int V_z dt. \quad (7)$$

The voltage across the inductor is related to the electric field as

$$V_z = \int E_z dl \simeq \Delta z E_z. \quad (8)$$

and the current to the current density by

$$I_{Lz} = \iint J_{Lz} dS \simeq \Delta x \Delta y J_{Lz}. \quad (9)$$

At the time step of $t = (n + 1/8)\Delta t$, the voltage and current characteristic equations of the lumped inductor are discussed through three different formulations: the explicit, the semi-implicit, and the implicit schemes.

$$\text{Explicit Scheme: } I_{Lz}^{n+1/8} = \frac{1}{L} \left(\frac{\Delta t}{4} \sum_{k=0}^{4n} V_z^{k/4} \right) = \frac{\Delta t \Delta z}{4L} \sum_{k=0}^{4n} E_z^{k/4} \quad (10a)$$

$$\begin{aligned} \text{Semi-Implicit Scheme: } I_{Lz}^{n+1/8} &= \frac{1}{L} \left(\frac{\Delta t}{4} \sum_{k=0}^{4n} V_z^{(2k+1)/8} \right) \\ &= \frac{\Delta t \Delta z}{4L} \frac{1}{2} \left(2 \sum_{k=0}^{4n} E_z^{k/4} + E_z^{n+1/4} \right) \quad (10b) \end{aligned}$$

$$\text{Implicit Scheme: } I_{Lz}^{n+1/8} = \frac{1}{L} \left(\frac{\Delta t}{4} \sum_{k=0}^{4n+1} V_z^{k/4} \right) = \frac{\Delta t \Delta z}{4L} \sum_{k=0}^{4n+1} E_z^{k/4}. \quad (10c)$$

The difference between (10a) and (10c) is that, in the latter expression, the summation runs up to $E_z^{n+1/4}$.

3. NUMERICAL STABILITY ANALYSIS

This section analyzes the stability of the SS4-FDTD method including lumped inductors. Since it is difficult to analyze the magnitudes of the eigenvalues of the updating matrix, the Fourier method, which has been used to study the stability of the SS4-FDTD method in [22], is not suitable here, and therefore, another stability analysis method based on von Neumann's theory [35] is adopted to prove the numerical stability, which has also been applied to the stability analysis of the extended FDTD method [29].

Theoretically, at each sub-step, when the extended SS4-FDTD method is unconditionally stable. Then, it can be generated that the extended SS4-FDTD method is unconditionally stable in a total time step. Otherwise, the extended SS-FDTD method is conditionally stable. Now the numerical stability in sub-step 1 is analyzed first, and then the numerical stability in other sub-steps can be obtained by using the similar method.

Based on the von Neumann method, a Fourier series expansion of the error function at the mesh node at a given time instant $t = n\Delta t$ is

considered. Due to linearity, only a single term of this expansion needs to be considered, i.e.,

$$f^n(i, j, k) = f_0 Z^n \exp [j(i\Delta x k_x + j\Delta y k_y + k\Delta z k_z)]. \quad (11)$$

where f_0 is a complex amplitude; indexes i, j, k denote the position of the nodes in the mesh; $\Delta x, \Delta y$ and Δz are the sizes of the discretization cell; k_x, k_y and k_z are the wave numbers of the discrete modes in the x -, y -, and z -directions, respectively. Z is the amplification factor, which gives the growth of the error in a time iteration, i.e., $f^{n+1}(i, j, k) = Z f^n(i, j, k)$.

By substituting (11) into (5a)–(5f), after a series of algebraic manipulations, the following equations can be generated.

$$(Z^{1/8} - Z^{-1/8})E_{x0} = \frac{\Delta t}{4\varepsilon} \frac{-2j \sin(k_y \Delta y / 2)}{\Delta y} (Z^{1/8} + Z^{-1/8}) H_{z0} \quad (12a)$$

$$(Z^{1/8} - Z^{-1/8})E_{y0} = \frac{\Delta t}{4\varepsilon} \frac{-2j \sin(k_z \Delta z / 2)}{\Delta z} (Z^{1/8} + Z^{-1/8}) H_{x0} \quad (12b)$$

$$(Z^{1/8} - Z^{-1/8})E_{z0} = \frac{\Delta t}{4\varepsilon} \frac{-2j \sin(k_x \Delta x / 2)}{\Delta x} (Z^{1/8} + Z^{-1/8}) H_{y0} - \frac{\Delta t}{4\varepsilon} \frac{I_{z0}}{\Delta x \Delta y} \quad (12c)$$

$$(Z^{1/8} - Z^{-1/8})H_{x0} = \frac{\Delta t}{4\mu} \frac{-2j \sin(k_z \Delta z / 2)}{\Delta z} (Z^{1/8} + Z^{-1/8}) E_{y0} \quad (12d)$$

$$(Z^{1/8} - Z^{-1/8})H_{y0} = \frac{\Delta t}{4\mu} \frac{-2j \sin(k_x \Delta x / 2)}{\Delta x} (Z^{1/8} + Z^{-1/8}) E_{z0} \quad (12e)$$

$$(Z^{1/8} - Z^{-1/8})H_{z0} = \frac{\Delta t}{4\mu} \frac{-2j \sin(k_y \Delta y / 2)}{\Delta y} (Z^{1/8} + Z^{-1/8}) E_{x0}. \quad (12f)$$

Substituting the voltage and current characteristic equations of the lumped inductor into (11), we can obtain the relationship of the amplitudes I_{L0} and E_{z0} . Then, a characteristic polynomial $S(Z)$ is obtained by replacing the relation into (12a) and (12f), (12b) and (12d), (12c) and (12e). Based on the von Neumann method, for a finite-difference scheme to be stable, all the roots Z_i of the stability polynomial $S(Z)$ must be inside or on the unit circle in the Z -plane, i.e., $|Z_i| \leq 1$.

By a series of analysis, $S(Z)$ is a second order polynomial in $Z^{1/4}$, and let $r = Z^{1/4}$, we have $S(r) = a_2 r^2 + a_1 r + a_0$. To ensure that a finite-difference scheme will be stable, the roots of $S(r)$ must lie inside or on the unit circle in the R -plane, i.e., $|r_i| \leq 1$. This must satisfy three algebraic inequalities:

$$a_2 \geq |a_0|, \quad S(1) \geq 0, \quad S(-1) \geq 0. \quad (13)$$

For E_x and H_z , substituting (12f) into (12a), the coefficients of the polynomial $S(r)$ are given by

$$a_2 = 1 + bdP_y^2, \quad a_1 = -2 + 2bdP_y^2, \quad a_0 = 1 + bdP_y^2.$$

where $b = \Delta t / (4\varepsilon)$, $d = \Delta t / (4\mu)$, $P_\alpha = -2 \sin(k_\alpha \Delta_\alpha / 2) / \Delta_\alpha$, $\alpha = x, y$, or z .

Then, all of the coefficients satisfy the inequalities (13), so the formulation of E_x and H_z is unconditionally stable.

For E_y and H_x , substituting (12d) into (12b), the coefficients of the polynomial $S(r)$ are given by

$$a_2 = 1 + bdP_z^2, \quad a_1 = -2 + 2bdP_z^2, \quad a_0 = 1 + bdP_z^2.$$

Also, all of the coefficients satisfy the inequalities (13), so the formulation of E_y and H_x is unconditionally stable.

Now, the stability of the formulation of E_z and H_y will be analyzed as follows. Substituting the error function of device current and electric field into the Equations (10a)–(10c), the following formulations are generated.

$$\text{Explicit Scheme : } \quad (Z^{1/8} - Z^{-1/8})I_{L0} = \frac{\Delta t \Delta z}{4L} E_{z0} \quad (14a)$$

$$\begin{aligned} \text{Semi-Implicit Scheme : } \quad (Z^{1/8} - Z^{-1/8})I_{L0} &= \frac{\Delta t \Delta z}{8L} Z^{1/8} \\ &\quad (Z^{1/8} + Z^{-1/8}) E_{z0} \end{aligned} \quad (14b)$$

$$\text{Implicit Scheme : } \quad (Z^{1/8} - Z^{-1/8})I_{L0} = \frac{\Delta t \Delta z}{4L} Z^{1/4} E_{z0}. \quad (14c)$$

Similarly, the polynomial $S(r)$ of the computation of E_z and H_y can be obtained after replacing the Equations (14a)–(14c) into the Equations (12c) and (12e).

3.1. Explicit Scheme

The coefficients of $S(r)$ for this scheme are given by

$$a_2 = 1 + bdP_x^2, \quad a_1 = -2 + 2bdP_x^2 + b \frac{\Delta t \Delta z}{4 \Delta x \Delta y L}, \quad a_0 = 1 + bdP_x^2.$$

In order to fulfill $|r_i| \leq 1$, according to the inequalities (13), the following stability condition must be verified.

$$\Delta t \leq 8 \sqrt{LC_c}. \quad (15)$$

where $C_c = \varepsilon \Delta x \Delta y / \Delta z$ is the cell capacitance. The inequality shows that this scheme is conditionally stable depending on the value of the

inductance and the mesh of the size. For this scheme, $S(r)$ is symmetric ($a_2 = a_0$), thus, if r_i is one of its roots, r_i^{-1} is also a root; consequently, as long as (15) is verified, we have $|r_{1,2}| = 1$ and, therefore, this scheme is non-dissipative.

3.2. Semi-implicit Scheme

For this scheme, the coefficients of the stability polynomial are given by

$$a_2 = 1 + bdP_x^2 + b \frac{\Delta t \Delta z}{8\Delta x \Delta y L}, \quad a_1 = -2 + 2bdP_x^2 + b \frac{\Delta t \Delta z}{8\Delta x \Delta y L}, \quad a_0 = 1 + bdP_x^2.$$

Here, all of these coefficients meet the inequalities (13), so the semi-implicit scheme is unconditionally stable.

3.3. Implicit Scheme

Similarly, the coefficients of the polynomial $S(r)$ are given by

$$a_2 = 1 + bdP_x^2 + b \frac{\Delta t \Delta z}{4\Delta x \Delta y L}, \quad a_1 = -2 + 2bdP_x^2, \quad a_0 = 1 + bdP_x^2.$$

By examining these coefficients, it is found that all of the inequalities (13) are met, so the implicit scheme of the lumped inductor is also unconditionally stable.

4. NUMERICAL ERROR ANALYSIS

Since it is difficult to analyze the magnitudes of the eigenvalues of the updating matrix, the Fourier method which has been used to study the dispersion of the SS4-FDTD [22], is not suitable here, and therefore, by using a circuital viewpoint [2], the numerical impedance of lumped inductors to be defined, and the numerical error of the extended SS4-FDTD method with a lumped inductor is analyzed through three different schemes.

As a starting point, we consider the circuital form-Norton equivalent circuit-of (5c) in the z -direction in sub-step 1, the similar formulations in other sub-steps can be obtained, which are also shown as follows.

$$\frac{4C_c}{\Delta t} \left(V_z^{n+1/4} - V_z^n \right) + I_{Lz}^{n+1/8} = I_{hy}^{n+1/4} + I_{hy}^n \quad (16a)$$

$$\frac{4C_c}{\Delta t} \left(V_z^{n+2/4} - V_z^{n+1/4} \right) + I_{Lz}^{n+3/8} = -I_{hx}^{n+2/4} - I_{hx}^{n+1/4} \quad (16b)$$

$$\frac{4C_c}{\Delta t} \left(V_z^{n+3/4} - V_z^{n+2/4} \right) + I_{Lz}^{n+5/8} = I_{hy}^{n+3/4} + I_{hy}^{n+2/4} \quad (16c)$$

$$\frac{4C_c}{\Delta t} \left(V_z^{n+1} - V_z^{n+3/4} \right) + I_{Lz}^{n+7/8} = -I_{hx}^{n+1} - I_{hx}^{n+3/4}. \quad (16d)$$

where I_{hx} and I_{hy} are the part of total current through the FDTD cell introduced by magnetic fields H_x and H_y , respectively. I_{Lz} is the current flowing through the lumped inductor, and V_z is the voltage.

By using the von Neumann method, substituting the voltage and current characteristic equation of the lumped inductor into (11), transforming (16a)–(16d), the following relations are generated.

$$\frac{4C_c}{\Delta t} \left(Z^{1/8} - Z^{-1/8} \right) V_{z0} + I_{Lz0} = \left(Z^{1/8} + Z^{-1/8} \right) I_{hy0} \quad (17a)$$

$$\frac{4C_c}{\Delta t} \left(Z^{1/8} - Z^{-1/8} \right) V_{z0} + I_{Lz0} = - \left(Z^{1/8} + Z^{-1/8} \right) I_{hx0}. \quad (17b)$$

and let the total current $I_z = I_{hy} - I_{hx}$, combining (17a) and (17b), the following formulation can be arrived.

$$2 \frac{4C_c}{\Delta t} \left(Z^{1/8} - Z^{-1/8} \right) V_{z0} + 2I_{Lz0} = \left(Z^{1/8} + Z^{-1/8} \right) I_{z0}. \quad (18)$$

where V_{z0} and I_{z0} denote the amplitudes of voltage and current. By simply letting $Z = e^{j\omega\Delta t}$, the above equation can be expressed as

$$I_{z0} = V_{z0} (1/Z_c + 1/Z_e). \quad (19)$$

where $Z_c = [8C_c j \tan(\omega\Delta t/8)/\Delta t]^{-1}$, and

$$Z_e = \left(Z^{1/8} + Z^{-1/8} \right) / 2 \cdot V_{z0} / I_{Lz0}. \quad (20)$$

are identified as the numerical impedances associated to the cell capacitance and to the lumped inductor, respectively.

Then, by substituting (14a)–(14c) into the expression of Z_e , the numerical results of the lumped inductor for three different schemes can be obtained.

4.1. Explicit Scheme

According to (20), the numerical impedance of the lumped inductor can be given by

$$Z_e = \frac{4j}{\Delta t} \sin \left(\frac{\omega\Delta t}{4} \right) L. \quad (21)$$

From the above expression, it can be seen that the real part of this expression is zero, and this scheme is non-dissipative.

4.2. Semi-implicit Scheme

For this scheme, the numerical impedance of the lumped inductor is

$$Z_e = \frac{8}{\Delta t} \sin^2\left(\frac{\omega\Delta t}{8}\right) L + j \frac{4}{\Delta t} \sin\left(\frac{\omega\Delta t}{4}\right) L. \quad (22)$$

Obviously, Z_e contains the loss real part, so this scheme is dissipative, and the dissipative nature of the lumped inductor can be replaced by an equivalent circuit consisting of an inductance and a series resistance $R_{si} = 8 \sin^2(\omega\Delta t/8)L/\Delta t$.

4.3. Implicit Scheme

For this scheme, the numerical impedance of the lumped inductor is given by

$$Z_e = \frac{4}{\Delta t} \sin^2\left(\frac{\omega\Delta t}{4}\right) L + j \frac{2}{\Delta t} \sin\left(\frac{\omega\Delta t}{2}\right) L. \quad (23)$$

Similarly, Z_e also contains the real part of loss. Similar to the semi-implicit scheme, the numerical equivalent circuit of the lumped inductor is an inductor in parallel with a resistor of resistance $R_i = 4 \sin^2(\omega\Delta t/4)L/\Delta t$. It can be observed that, when the time step is set smaller, the numerical dissipative nature of the lumped inductor also decreases.

5. NUMERICAL RESULTS

In order to illustrate the validity of the stability conditions and dispersion error characteristic derived in the preceding sections, the

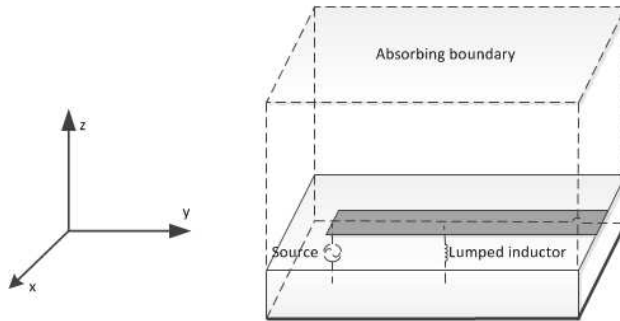


Figure 1. Configuration of microstrip structure with the lumped inductor.

stability of the explicit, the semi-implicit, and the implicit schemes are studied. Then, the extended SS4-FDTD method is utilized to simulate a microstrip structure with a lumped inductor as shown in Figure 1. The entire computation domain is divided into $30 \times 100 \times 15$ in x -, y - and z -directions, and cell sizes $\Delta x = \Delta y = \Delta z = 0.15$ mm. The thickness of the dielectric plane is $1\Delta z$, and the dielectric constant $\epsilon_r = 2.55$. The dimension of the metal strip is $2\Delta x \times 90\Delta y$. Mur's first-order absorbing boundary condition is applied on the truncated boundary to absorb out-going waves except for the $z = 0$ plane. In addition, for the $z = 0$ plane, it is terminated with perfect electric conducting (PEC) boundary. Therefore, on the PEC outer boundary of the FDTD space lattice, the tangential electric fields remain zero for all time steps. A voltage source is connected to one termination of the metal strip, which is $10\Delta y$ apart from the absorbing boundary. At the node $(15\Delta x, 50\Delta y)$, a lumped inductor of inductance $L = 1$ pH is used between the metal strip and the infinite ground plane, as shown in Figure 1. $\Delta t_{\max} = 8\sqrt{LC_c}$ is the maximum of the Δt in the explicit scheme in (15). Here, CFLN is used: it is defined as the ratio between the time step taken and the maximum time step limit of the explicit scheme, i.e., $\text{CFLN} = \Delta t / \Delta t_{\max}$.

For the explicit scheme, four different simulations have been performed: CFLN = 0.2, 0.5, 0.9, 1.01. Figure 2 shows the electric field at the node $(15\Delta x, 50\Delta y)$, as a function of the time step. It can be seen that the simulations with CFLN = 0.2, 0.5, 0.9 remains stable during the whole period of time; whereas, when CFLN = 0.9, the error of the result is becoming larger, it can be explained by a simple

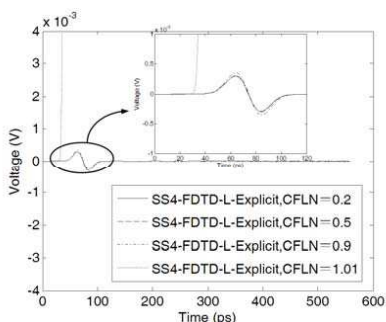


Figure 2. Voltage across the lumped inductor of the extended SS4-FDTD method for the explicit scheme.

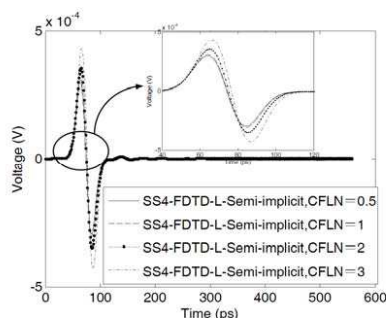


Figure 3. Voltage across the lumped inductor of the extended SS4-FDTD method for the semi-implicit scheme.

argument. $CFLN = 0.9$ closes to the critical point of the stability of the explicit scheme and, therefore, the result with $CFLN = 0.9$ is stable, though the result with $CFLN = 0.9$ is not accurate. On the other hand, when $CFLN = 1.01$, the field begins to increase without bound, thus, it is unstable.

For the semi-implicit scheme and implicit scheme, four different simulations have been performed: $CFLN = 0.5, 1, 2, 3$ or 4 . Figures 3 and 4 show the electric fields at the node $(15\Delta x, 50\Delta y)$, as a function of the time step. From Figure 3, the semi-implicit scheme is stable with $CFLN = 1, 2$, and 3 , so the extended SS4-FDTD methods with the semi-implicit scheme is unconditionally stable. However, the error of the result with the semi-implicit scheme increases as $CFLN$ increases, when $CFLN = 3$, the error of the result with the semi-implicit scheme is becoming larger. On the other hand, as can be seen from Figure 4, the implicit scheme is stable with $CFLN = 1, 2, 4$, and the implicit scheme is unconditionally stable. In addition, the error of the result with the implicit scheme increases as $CFLN$ increases. Nevertheless, the increase of the error of the result with the implicit scheme is much less pronounced than that of the changes in Figure 3. Specifically, the result of the extended SS4-FDTD method with the implicit scheme of $CFLN = 4$ is in good agreement with the result of $CFLN = 1$. Therefore, among the explicit, the semi-implicit and the implicit schemes, the implicit scheme exhibits good accuracy while preserving the unconditionally-stable.

In order to show the validity of the analytical expressions for Z_L obtained for three schemes under study, Z_L directly from the SS4-FDTD simulations are computed. To this end, a procedure consisting

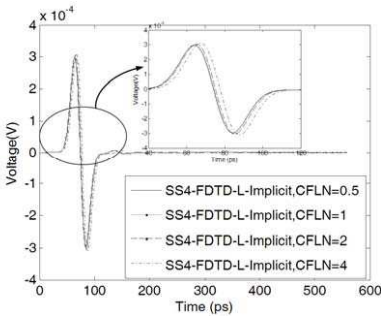


Figure 4. Voltage across the lumped inductor of the extended SS4-FDTD method for the implicit scheme.

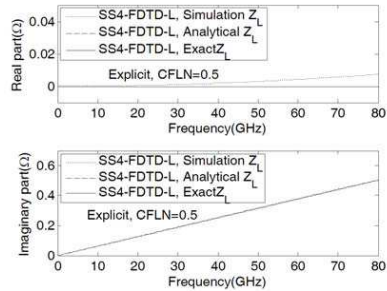


Figure 5. Lumped inductor impedance of the extended SS4-FDTD method for the explicit scheme with $L = 1$ pH.

of two different simulations is used.

Firstly, a plane-wave propagation through an unloaded spatial region consisting of $30 \times 100 \times 15$ cells of sizes $\Delta x = \Delta y = \Delta z = 0.15$ mm. At a specific node, the current $I_z^{n+1}(i, j, k + 1/2)$ and the voltage $V_z^{n+1}(i, j, k + 1/2)$ employing the following expressions are recorded:

$$I_z \Big|_{i,j,k+1/2}^{n+1} = \left(H_y \Big|_{i+1/2,j,k+1/2}^{n+1} - H_y \Big|_{i-1/2,j,k+1/2}^{n+1} \right) \cdot \Delta y - \left(H_x \Big|_{i,j+1/2,k+1/2}^{n+1} - H_x \Big|_{i,j-1/2,k+1/2}^{n+1} \right) \cdot \Delta x \quad (24a)$$

$$V_z \Big|_{i,j,k+1/2}^{n+1} = E_z \Big|_{i,j,k+1/2}^{n+1} \cdot \Delta z. \quad (24b)$$

As a post-processing task, the impedance associated to the cell capacitance is computed as

$$Z_c = \tilde{V}_z / \tilde{I}_z = DFT(V_z^{n+1}) / DFT(I_z^{n+1}). \quad (25)$$

Secondly, node $(i, j, k + 1/2)$ is loaded with a lumped inductor and a new simulation is performed. Repeating the procedure described above, the total numerical impedance of the loaded case Z_T is computed.

Finally, Z_e is calculated as

$$Z_e = (1/Z_T - 1/Z_c)^{-1}. \quad (26)$$

Figure 5 compares the analytical expression of Z_e (21) with the data obtained by the SS4-FDTD simulations, with the exact impedance $Z_e = j\omega L$ for the explicit scheme with $L = 1$ pH. The CFLN value in these calculations is 0.5 and the results are shown up to 80 GHz, which corresponds to a spatial resolution of 25 cells per wavelength in free space. It can be observed that the SS4-FDTD results are in good agreement with (21). Therefore, the explicit scheme provides values of imaginary part that are in good agreement with the exact ones.

The comparison made in Figure 5 is repeated in Figures 6 and 7 for the semi-implicit and the implicit schemes, respectively. In these figures, the value of the inductance is maintained as shown in Figure 5. Again, for the imaginary part, the analytical expressions Z_L of the SS4-FDTD results are in good agreement with the exact ones. From Figure 6, for the semi-implicit scheme, when CFLN = 1, the simulation result of the SS4-FDTD method is in good agreement with the analytical expression of Z_L . However, the error between the simulation result and the analytical expression of Z_L is becoming larger as the CFLN increases. Subsequently, from Figure 7, for the implicit scheme, the simulation result of SS4-FDTD method keeps a good agreement with the analytical expression of Z_L as the CFLN

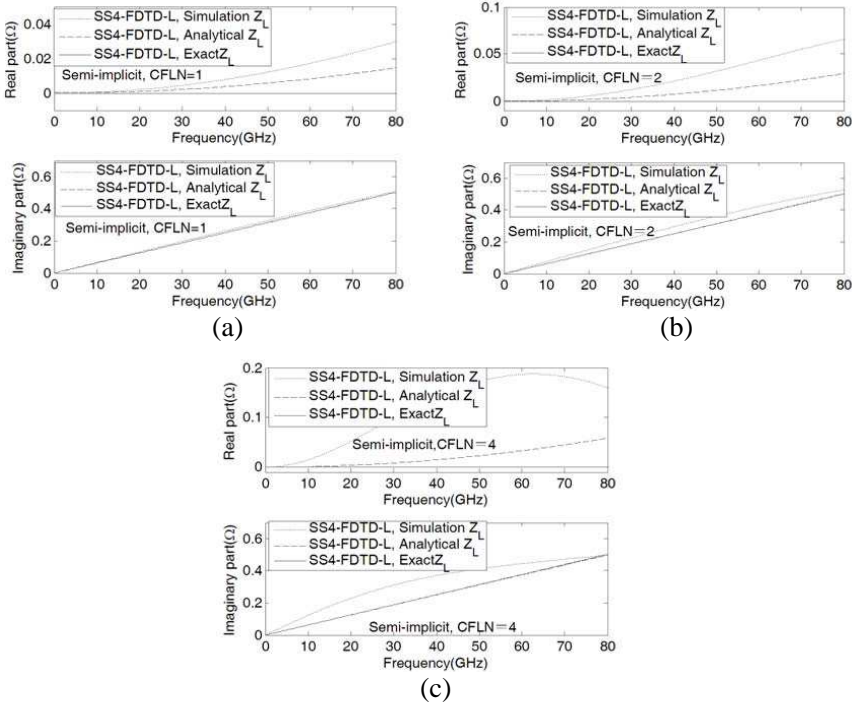


Figure 6. Lumped inductor impedance of the extended SS4-FDTD method for the semi-implicit scheme with $L = 1$ pH. (a) CFLN = 1. (b) CFLN = 2. (c) CFLN = 4.

increases. On the other hand, for the real part and the semi-implicit scheme in Figure 6, when the values of the CFLN and frequency are small, the simulation result is close to the exact one. However, as the values of the CFLN and frequency increase, the error between the simulation and the exact value increases. This is most likely due to the fact that the real part of the simulation is a resistance $R_{si} = 8 \sin^2(\omega\Delta t/8)L/\Delta t$ in (22), whereas, for the exact value, the real part is zero. Moreover, for the implicit scheme, the real part in Figure 7 has the similar characteristic. Specifically, the real part of the simulation is a resistance $R_i = 4 \sin^2(\omega\Delta t/4)L/\Delta t$ in (23); however, for the exact value, the real part is also zero. Therefore, the values of CFLN and frequency are set larger, the error between the simulation and the exact value increases.

Comparing the results obtained by three schemes under study, the implicit scheme exhibits also good accuracy added to its inherent unconditional stability. Therefore, it is observed that the implicit scheme exhibits the best accuracy of all.

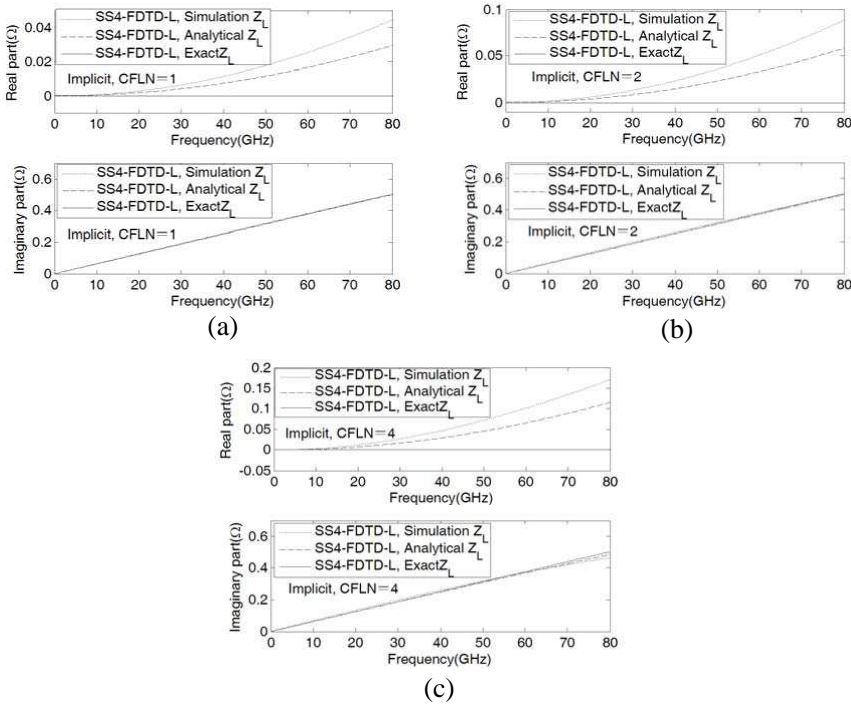


Figure 7. Lumped inductor impedance of the extended SS4-FDTD method for the implicit scheme with $L = 1$ pH. (a) CFLN = 1. (b) CFLN = 2. (c) CFLN = 4.

6. CONCLUSION

The stability and numerical error analysis of the extended SS4-FDTD method including the lumped inductor have been studied in this paper. Three finite-difference schemes have been analyzed, which are the explicit, the semi-implicit, and the implicit schemes. Furthermore, the stability analysis of the formulations has been studied by using the von Neumann method. Specifically, the theoretical stability analysis shows that the explicit scheme is conditionally stable, and the stability criterion depends on both the values of the inductor and the mesh sizes, whereas the semi-implicit and the implicit schemes are unconditionally stable. Moreover, the closed-form numerical error expressions have been derived for each scheme based on the circuitual viewpoint. From the standpoint of accuracy, the explicit scheme has a non-dissipative nature and exhibits the best accuracy of all. However, in practice, this

fact does not represent any advantage because a restrictive stability condition must be employed in this scheme. The semi-implicit and the implicit schemes are slightly dissipative. Finally, a microstrip circuits including a lumped inductor has been simulated to show the validity of the theoretical results. Comparing the results obtained by three schemes under study, the implicit scheme exhibits the best accuracy of all.

ACKNOWLEDGMENT

This work was supported by the National Natural Science Foundation of China (61171029) and the Program of State Key Laboratory of Millimeter Waves (K201102), Southeast of University.

REFERENCES

1. Yee, K. S., "Numerical solution of initial boundary value problems involving Maxwell's equations in isotropic media," *IEEE Trans. Antennas Propag.*, Vol. 14, No. 3, 302–307, May 1966.
2. Taflove, A. and S. C. Hagness, *Computational Electrodynamics: The Finite-difference Time-domain Method*, 2nd Edition, Artech House, Boston, MA, 2000.
3. Namiki, T., "A new FDTD algorithm based on alternating-direction implicit method," *IEEE Trans. Microwave Theory Tech.*, Vol. 47, No. 10, 2003–2007, Oct. 1999.
4. Zheng, F., Z. Chen, and J. Zhang, "Toward the development of a three-dimensional unconditionally stable finite-difference time-domain method," *IEEE Trans. Microwave Theory Tech.*, Vol. 48, No. 9, 1550–1558, Sep. 2000.
5. Tay, W. C., D. Y. Heh, and E. L. Tan, "GPU-accelerated fundamental ADI-FDTD with complex frequency shifted convolutional perfectly matched layer," *Progress In Electromagnetics Research M*, Vol. 14, 177–192, 2010.
6. Gan, T. H. and E. L. Tan, "Stability and dispersion analysis for three-dimensional (3-D) leapfrog ADI-FDTD method," *Progress In Electromagnetics Research M*, Vol. 23, 1–12, 2012.
7. Sun, G. and C. W. Trueman, "Approximate Crank-Nicolson schemes for the 2-D finite-difference time-domain method for TEz waves," *IEEE Trans. Antennas Propag.*, Vol. 52, No. 11, 2963–2972, Nov. 2004.
8. Sun, G. and C. W. Trueman, "Efficient implementations of the Crank-Nicolson scheme for the finite-difference time-domain

- method,” *IEEE Trans. Microw. Theory Tech.*, Vol. 54, No. 5, 2275–2284, May 2006.
9. Rouf, H. K., F. Costen, S. G. Garcia, and S. Fujino, “On the solution of 3-D frequency dependent Crank-Nicolson FDTD scheme,” *Journal of Electromagnetic Waves and Applications*, Vol. 23, No. 16, 2163–2175, Jan. 2009.
 10. Xu, K., Z. Fan, D. Z. Ding, and R.-S. Chen, “GPU accelerated unconditionally stable Crank-Nicolson FDTD method for the analysis of three-dimensional microwave circuits,” *Progress In Electromagnetics Research*, Vol. 102, 381–395, 2010.
 11. Fu, W. and E. L. Tan, “Development of split-step FDTD method with higher-order spatial accuracy,” *Electron. Lett.*, Vol. 40, No. 20, 1252–1253, Sep. 2004.
 12. Fu, W. and E. L. Tan, “Compact higher-order split-step FDTD method,” *Electron. Lett.*, Vol. 41, No. 7, 397–399, Mar. 2005.
 13. Shibayama, J., M. Muraki, J. Yamauchi, and H. Nakano, “Efficient implicit FDTD algorithm based on locally one-dimensional scheme,” *Electron. Lett.*, Vol. 41, No. 19, 1046–1047, Sep. 2005.
 14. Do Nascimento, V. E., J. A. Cuminato, F. L. Teixeira, and B.-H. V. Borges, “Unconditionally stable finite-difference time-domain method based on the locally-one-dimensional technique,” *Proc. XXII Simpósio Brasileiro de Telecomunicações*, 288–291, Campinas, SP, Brazil, Sep. 2005.
 15. Liang, F. and G. Wang, “Fourth-order locally one-dimensional FDTD method,” *Journal of Electromagnetic Waves and Applications*, Vol. 22, Nos. 14–15, 2035–2043, Jan. 2008.
 16. Tan, E. L., “Unconditionally stable LOD-FDTD method for 3-D Maxwell’s equations,” *IEEE Microw. Wireless Compon. Lett.*, Vol. 17, No. 2, 85–87, Feb. 2007.
 17. Ahmed, I., E. K. Chua, E. P. Li, and Z. Chen, “Development of the three-dimensional unconditionally-stable LOD-FDTD method,” *IEEE Trans. Antennas Propag.*, Vol. 56, No. 11, 3596–3600, Nov. 2008.
 18. Kong, Y.-D. and Q.-X. Chu, “Reduction of numerical dispersion of the six-stages split-step unconditionally-stable FDTD method with controlling parameters,” *Progress In Electromagnetics Research*, Vol. 122, 175–196, 2012.
 19. Chu, Q. X. and Y. D. Kong, “High-order accurate FDTD method based on split-step scheme for solving Maxwell’s equations,” *Microwave. Optical Technol. Lett.*, Vol. 51, No. 2, 562–565, Feb. 2009.

20. Chu, Q. X. and Y. D. Kong, "Three new unconditionally-stable FDTD methods with high-order accuracy," *IEEE Trans. Antennas Propag.*, Vol. 57, No. 9, 2675–2682, Sep. 2009.
21. Kong, Y. D. and Q. X. Chu, "Unconditionally-stable FDTD methods with high-order accuracy in two and three dimensions," *IET Microwaves, Antennas Propag.*, Vol. 4, No. 10, 1605–1616, Nov. 2010.
22. Kong, Y. D. and Q. X. Chu, "High-order split-step unconditionally-stable FDTD methods and numerical analysis," *IEEE Trans. Antennas Propag.*, Vol. 59, No. 9, 3280–3289, Sep. 2011.
23. Pereda, J. A., F. Alimenti, P. Mezzanotte, L. Roselli, and R. Sorrentino, "A new algorithm for the incorporation of arbitrary linear lumped networks into FDTD simulators," *IEEE Trans. Microw. Theory Tech.*, Vol. 47, No. 6, 943–949, Jun. 1999.
24. Chen, Z.-H. and Q.-X. Chu, "FDTD modeling of arbitrary linear lumped networks using piecewise linear recursive convolution technique," *Progress In Electromagnetics Research*, Vol. 73, 327–341, 2007.
25. Su, D. Y., D.-M. Fu, and Z.-H. Chen, "Numerical modeling of active devices characterized by measured S -parameters in FDTD," *Progress In Electromagnetics Research*, Vol. 80, 381–392, 2008.
26. Silva-Macêdo, J. A., M. A. Romero, and B.-H. V. Borges, "An extended FDTD method for the analysis of electromagnetic field rotators and cloaking devices," *Progress In Electromagnetics Research*, Vol. 87, 183–196, 2008.
27. Thiel, W. and L. P. B. Katehi, "Some aspects of stability and numerical dissipation of the finite-difference time-domain (FDTD) technique including passive and active lumped elements," *IEEE Trans. Microw. Theory Tech.*, Vol. 50, No. 9, 2159–2165, Sep. 2002.
28. Kung, F. and H. T. Chuah, "Stability of classical finite-difference time-domain (FDTD) formulation with nonlinear elements — A new perspective," *Progress In Electromagnetics Research*, Vol. 42, 49–89, 2003.
29. Pereda, J. A., A. Vegas, and A. Prieto, "Study on the stability and numerical dispersion of the FDTD technique including lumped inductors," *IEEE Trans. Microw. Theory Tech.*, Vol. 52, No. 3, 1052–1058, Mar. 2004.
30. Fu, W. and E. L. Tan, "Unconditionally stable FDTD technique including passive lumped elements," *International RF and Microwave Conference Proceedings*, 277–280, Putrajaya,

- Malaysia, Sep. 2006.
31. Fu, W. and E. L. Tan, "Unconditionally stable ADI-FDTD method including passive lumped elements," *IEEE Trans. Electromagnetic Compatibility*, Vol. 48, No. 4, 661–668, Nov. 2006.
 32. Chu, Q. X. and Z. H. Chen, "Numerical dispersion of the ADI-FDTD technique including lumped models," *IEEE MTT-S Int. Micro. Sym. Dig.*, 729–732, Honolulu, United States, Jun. 2007.
 33. Lin, G. and Y. G. Zhou, "Extending the three-dimensional LOD-FDTD method to lumped load and voltage source with impedance," *International Conference on Microwave Technology and Computational Electromagnetics*, 341–343, Beijing, China, 2009.
 34. Lee, J. and B. Fornberg, "A split step approach for the 3-D Maxwell's equations," *J. Comput. Appl. Math.*, No. 158, 485–505, Mar. 2003.
 35. Pereda, J. A., L. A. Vielva, A. Vegas, and A. Prieto, "Analyzing the stability of the FDTD technique by combining the von Neumann method with the Routh-Hurwitz," *IEEE Trans. Microw. Theory Tech.*, Vol. 49, No. 2, 377–381, Feb. 2001.